

ORIGINAL ARTICLE

Open Access



# Experimental study on the compression behavior of long timber column strengthened with the novel hybrid fiber sheets

Haoyu Wang<sup>1</sup>, Qing Chun<sup>1\*</sup>, Chengwen Zhang<sup>1</sup>, Shiyu Ma<sup>1</sup>, Guang Cao<sup>2</sup> and Qingchong Dong<sup>2</sup>

## Abstract

Long timber columns are widely used in traditional timber structures worldwide; however, many of them possess bearing capacity issues and have to be strengthened. The current study aims to develop the novel Hybrid fiber reinforced polymers (HFRP) sheets suitable for long timber columns. In the first stage, six HFRP sheets were designed, and the evaluation of these sheets was carried out by the tensile tests and the Scanning electron microscopy (SEM) tests. Secondly, for the compression test, two sets of 36 timber columns were designed utilizing six types of HFRP sheets. Finally, the effects of different sheet types and strengthening methods on the compressive performance of timber columns were investigated. The findings reveal that bidirectional HFRP sheets have excellent compressive performance for timber columns. In the case of using one-layer interval reinforcement, the bearing capacity can be increased by 22.27%, which is 12.15–17.81% higher than that of the unidirectional HFRP sheets. Compared with one-layer reinforcement, the two-layer reinforcement increased from 0.91% to 5.35%. The current study's findings are intended to provide an essential scientific foundation for the advancement of fiber-reinforced timber column technology and the preservation of the heritage of timber structures.

**Keywords** Long timber column, Hybrid fiber sheet, Mechanical properties, Compression test, Scanning electron microscopy

## Introduction

Timber is a widely implemented, sustainable, and environmentally friendly building material worldwide [1]. In addition, logs have been used as a traditional building material for thousands of years, and timber structures have a part in architectural heritage around the world, with examples of traditional Asian temples [2], and European churches [3, 4]. However, timber structures, which are a relic of history, were built long ago and have been affected by material aging, loading, biological corrosion, natural corrosion, fatigue effect, and

other adverse factors leading to consequences such as damage accumulation, reduced service life [5]. Replacing these damaged timber components with new ones is not always feasible because it does not meet the principle of authenticity [6] in conserving traditional structures, given the desire to preserve original parts. Therefore, there is increasing interest in research on adaptive repair techniques for older timber heritage components, such as fiber sheets for reinforcement [7, 8].

Fiber composites are particularly applicable for the repair and reinforcement of timber buildings since they are strong [9], lightweight, and their surface can be painted or coated with different coatings [10]; hence, maximum restoration in appearance is possible. The fibers used in these composites are mainly carbon fiber, glass fiber, aramid fiber, etc. These different fibers have their own advantages and disadvantages. Carbon fiber,

\*Correspondence:

Qing Chun  
cqj1979@163.com

<sup>1</sup> School of Architecture, Southeast University, Nanjing, China

<sup>2</sup> China State Construction Engineering Corporation, Beijing, China

for example, has the advantages of being lightweight and high strength, but the ductility is poor [11, 12]. Although aramid fiber exhibits very high toughness and elongation, it has relatively lower strength and higher cost compared with carbon fiber [13]. Glass fiber has strength and ductility between carbon fiber and aramid fiber, and it is fairly inexpensive, except for some special products [14–16]. In addition, basalt fibers [10, 17, 18], metal fibers [19], and natural fibers [15, 20] are other fiber types used. Blending design [21], including interply blending, intra-ply blending, etc., can mitigate the disadvantages of a single fiber and merge the advantages of multiple fibers [22]. A particular ratio blending of carbon fiber and aramid fiber, for instance, can ensure the production of fiber sheets with high strength and ductility characteristics at the same time.

In recent years, fiber materials have been widely used as reinforcement in structural members, especially concrete members [23, 24]. Additionally, in the literature, there are studies related to the flexural behavior [25, 26] or shear performance [8, 27] of fiber-reinforced timber beams and many applications of new fiber composites. This study aims to investigate a new reinforcement technique for timber columns. Therefore, the following literature mainly covers column reinforcement research.

Most of the research on fiber-reinforced timber columns has focused on short columns. For instance, Najm et al. [28] investigated the compressive performance improvement of Carbon fiber reinforced polymers (CFRP) reinforced short timber columns. The carbon fiber in the weft direction was found to increase the columns' strength, stiffness, and ductility while also reducing the material variability of the timber. Ouyang et al. [29] studied the nonlinear stability of Fiber-reinforced polymers (FRP) reinforced simply supported timber columns, and the results showed that the FRP reinforcement layer enhanced the ultimate bearing capacity of the columns. Xiong et al. [30] investigated the effect of fiber reinforcement on the compressive capacity of timber short columns and reported that the carbon fiber reinforcement had the potential to increase compressive bearing capacity by about 20%. Siha et al. [31] presented new fiber reinforcement methods for short timber columns, combining the CFRP and carbon fiber tendons. Dong et al. [32] compared the reinforcement impacts of Aramid fiber reinforced polymers (AFRP), CFRP, and Basalt fiber reinforced polymers (BFRP), considering the effect of knots on the bearing capacity of short timber columns. Lee et al. [33] compared the effect of CFRP external reinforcement to CFRP/Glass fiber reinforced polymers (GFRP) reinforcement or plate internal reinforcement and revealed that carbon fiber external reinforcement enhanced compressive bearing

capacity by roughly 7%. Dong et al. [34] investigated the compressive damage mode, bearing capacity, load–strain curve, ductility factor, and stiffness factor of FRP reinforced short timber columns and stated that FRP reinforcement could improve the compressive bearing capacity by 100.2%. Taheri et al. [35] conducted an axial compression test on three different lengths of glued timber columns reinforced by CFRP, and the direction of reinforcement was along the direction of timber fiber. Besides the effects of different length to slenderness ratios, different boundary conditions, and the length of FRP reinforcement were considered. The study's findings revealed that bending damage was the most prominent type of damage for long columns and that reinforcement in the middle bending region had a substantial impact on compressive bearing capacity, increasing it by up to 80%. Zhang et al. [36] investigated the damage pattern and the compressive bearing capacity improvement of long timber columns with longitudinal shrinkage cracks. The damage pattern of long timber columns was primarily bending damage, and the compressive bearing capacity was increased by around 20%, although the fiber reinforcement direction was transverse, according to the findings. In a study conducted by Lu et al. [37] on CFRP reinforced long columns under eccentric pressure, the results showed that the bearing capacity increased by approximately 24%.

To summarize, the gaps detected in the current studies in the literature are as follows: (1) The majority of fibers utilized in fiber-reinforced timber columns were single fibers, and interlaminar hybrid fiber sheets were rarely considered to increase the performance of the fiber sheet. (2) The majority of the research subjects were short timber columns, with only a few long column investigations. Short timber columns and long timber columns collapse in distinct ways. (3) The arrangement of fiber-reinforced long timber columns was unclear, and there was little discussion of the benefits and drawbacks of different reinforcement methods.

Based on the above investigations, this paper aims to examine a more suitable HFRP sheet for timber column reinforcement and compare the advantages and disadvantages of various reinforcement techniques. The current study offers the following solutions to fill the gaps mentioned above.

- (1) With the material property tests, a total of six different types of HFRP sheets were prepared and tested for material properties. Then, the micro-stress modes of the sheets at tensile fracture were obtained using the SEM analysis. The subsequent examination of compression testing was supported

through the comparison of tensile strength, elongation, and microscopic failure modes.

- (2) To investigate the effect of various sheets and the number of reinforcement layers, the first stage of the experiment employed six types of sheets with weft interval reinforcement. Then, the impact of various reinforcement methods was investigated in the second stage of the experiment.

## Materials and methods

### Material property tests

#### Fiber

Three types of reinforcing fiber were employed in the HFRP sheets in this experiment: carbon fiber, glass fiber, and aramid fiber. Although carbon fiber has excellent tensile strength, ductility and elongation performance are unsatisfactory. The basis of the superiority of aramid fiber is its high toughness performance, which also makes it the core material of bulletproof technology. However, the exorbitant price and relatively lower strength compared with carbon fiber clearly reveal the disadvantage of aramid fiber [21]. Glass fiber, on the other hand, has a moderate performance in terms of strength and toughness, and its cost is extremely low [22]. The matrix employed in this investigation is MR241 AB adhesive produced by MIRA company, Singapore. The A component of MR241 AB is epoxy resin, and the B component is modified amine. The material properties of the fiber rayon and matrix are presented in Table 1. A new kind of HFRP sheet with high strength and toughness can be obtained through the hybrid effect as the primary material for strengthening timber structures. A new kind of HFRP sheet with high strength and toughness can be obtained through the hybrid effect as the primary material for strengthening timber structures.

The above-mentioned fibers were used to design four different types of unidirectional HFRP sheets and two types of bidirectional HFRP sheets within this study. The warp fibers were proportionately placed and pre-tightened into a single layer fabric using wiring devices, pre-tighten and hot-press devices. The weft fiber

was then inserted before being thermoformed. The manufacturing equipment is shown in Fig. 1, and six types of fiber sheets are shown in Table 2.

Six types of HFRP sheets were utilized to produce tensile specimens in accordance with GB/T 3354-2014 [38], and each type of HFRP sheet was produced with six repeated specimens. The specimen size is shown in Fig. 2 and the tensile specimens are given in Fig. 3. It should be noted that the adhesive appeared blue after curing, thus the color of specimens had been changed. Carbon fiber appeared black, while glass fiber and aramid fiber absorbing the adhesive appeared light blue. These tensile specimens were tested after 24 h of curing at  $23 \pm 2$  °C and  $50 \pm 10\%$  relative humidity. A universal testing machine was used to perform the experimental study (Model CMT5504). The specimens were constantly loaded at 1 mm/min, and the load–strain curves of the specimens were periodically recorded.

The test results are presented in Table 3, where  $f_t$  represents tensile strength and  $\varepsilon$  represents elongation. The micro-structural investigation of the tensile failure specimens was further performed by SEM, as shown in Fig. 4.

As can be seen in Table 3, the tensile strengths of C2G1 and C1A2G1 were obtained lower compared to CFRP, by 15.11% and 7.36%, respectively. The tensile strength of C2A1G1 was measured as 5.98% higher than that of CFRP. Besides, the elongation of C2A1G1 and C1A2G1 was about twice as high as that of CFRP. In comparison to CFRP, there was a tendency to higher tensile strength and elongation for both bidirectional sheets.

From SEM micro-graphs, as shown in Fig. 4a, the fracture of CFRP was quite flat, and the fracture of carbon fiber filaments was flat and brittle. The epoxy matrix between the carbon fibers was damaged and fragmented. Figure 4b shows the fracture of the C2G1 specimen; the fracture of the fiber filaments was quite flat similar to CFRP, and the fracture was perpendicular to the member direction. In addition, it was detected that only some fibers were fractured, and the epoxy matrix between the fibers was damaged for the relevant situation. In this case, it can be assumed that the

**Table 1** Material properties of the fiber rayon and matrix

Fiber and matrix	Tensile strength/MPa	Elasticity (or tensile) modulus/GPa	Elongation/%	Density/g·cm <sup>-3</sup>
Carbon fiber (Toray T300–3 K)	3530	230	1.5	1.76
Aramid fiber (Kevlar 29)	1840	40–70	3.1	1.44
Glass fiber (JuShi e-glass 300tex)	2000–3000	30	2.0–3.0	2.58
MR241 AB	40	2.4	/	2.0

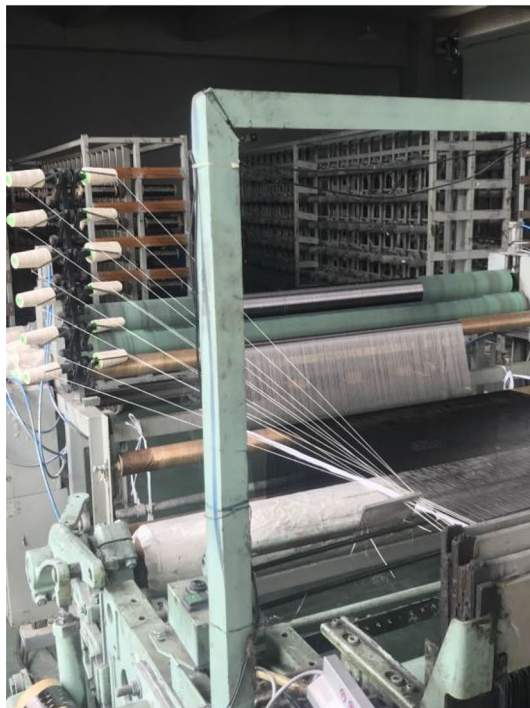




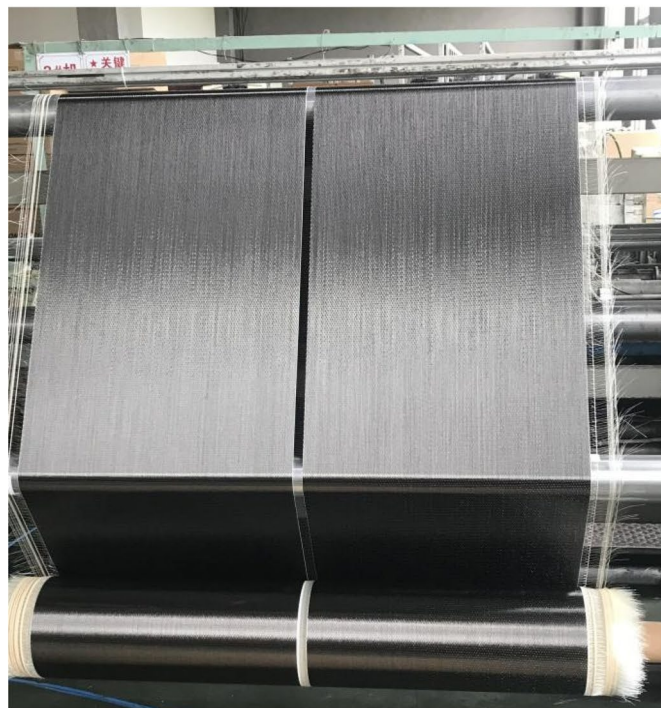
(a) Wiring devices (longitudinal)



(b) Pre-tighten and hot-press device



(c) Wiring device (latitudinal)



(d) Cloth roller device




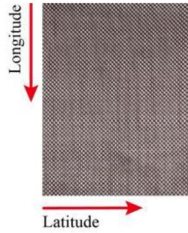

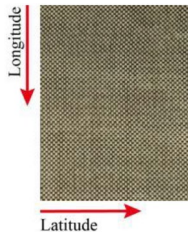
**Fig. 1** Manufacturing process

matrix is the first phase to reach the ultimate strain during the stretching process. As shown in Fig. 4c, under unidirectional force, the aramid filaments in the C1A2G1 specimen fractured scattered, and their fragments exhibit significant ductility, in contrast to the first two specimens, which were quite flat and perpendicular to the member direction. This may not be conducive for the specimen to subject unidirectional forces. The fiber arrangement at the fracture in Fig. 4d

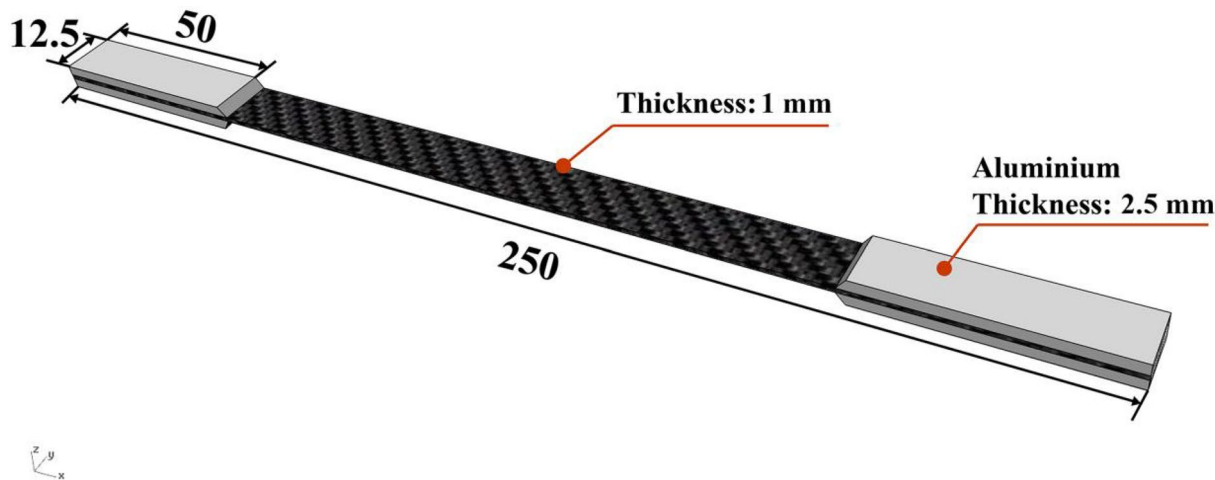
was of high tightness, which was more advantageous to the specimen's strength due to the reduced proportion of aramid fiber and the constraint of carbon fiber on both sides.

The results of bidirectional sheets are presented in Fig. 4e and f. In Fig. 4e, the fracture was mainly detected for longitudinal carbon fibers inside the red dashed box, and the fracture was very flat and consistent with the fracture behavior observed in CFRP. However, for

**Table 2** Design scheme of fiber sheet

Types of the fiber sheet	Photo of the sheet	Density/g·cm <sup>-3</sup>	Types of the fiber sheet	Photo of the sheet	Density/g·cm <sup>-3</sup>
Unidirectional CFRP		1.76	Unidirectional hybrid CFRP:AFRP:GFRP = 1:2:1 (abbreviated as C1A2G1)		1.80
Unidirectional hybrid CFRP:GFRP = 2:1 (abbreviated as C2G1)		2.03	Bidirectional hybrid Longitude CFRP Latitude GFRP (abbreviated as CoGa)		2.17
Unidirectional hybrid CFRP:AFRP:GFRP = 2:1:1 (abbreviated as C2A1G1)		1.88	Bidirectional hybrid Longitude CFRP Latitude AFRP (abbreviated as CoAa)		1.60

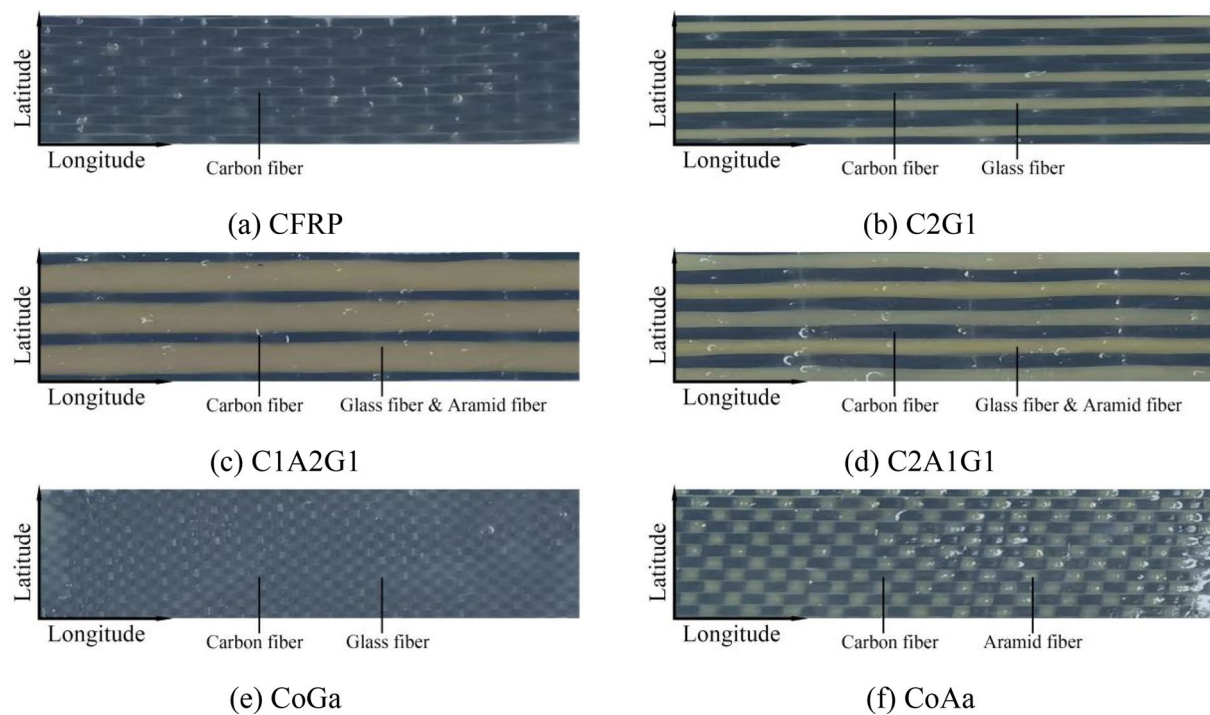
The fiber rayon density in both longitude and latitude directions is 6/cm



**Fig. 2** Dimension of the HFRP tensile specimens (unit: mm)

the CoAa specimen, fracture and deformation were more cluttered for the transverse aramid fibers in the red dashed box. Although this alteration in aramid fiber orientation increased the number of fibers involved in longitudinal stress loading, it also increased transverse damage. The accumulation of this damage caused

transverse matrix cracking and aramid fiber breaking, which eventually affected force loading. In summary, compared with CFRP, C2A1G1 exhibited the best tensile strength, ductility, and stress pattern summarized from SEM photos among these four unidirectional fiber sheets. Besides, C1A2G1 had higher



**Fig. 3** Photographs of tensile specimens

**Table 3** Material properties of hybrid fiber sheets

Material parameter	CFRP		C2G1		C1A2G1	
	Value	Coefficient of variation (%)	Value	Coefficient of variation (%)	Value	Coefficient of variation (5)
$f_t$	2607 MPa	4.3	2213 MPa	5.4	2415 MPa	7.6
$\varepsilon$	1.23%	6.28	1.49%	7.2	2.47%	5.2
Material parameter	C2A1G1		CoGa		CoAa	
	Value	Coefficient of variation (%)	Value	Coefficient of variation (%)	Value	Coefficient of variation (%)
$f_t$	2763 MPa	6.7	2922 MPa	15.3	2718 MPa	16.3
$\varepsilon$	2.05%	8.7	1.66%	17.9	1.72%	19.5

The variation coefficient of material parameters of bidirectional fabric is larger. This is because the production steps of bidirectional HFRP sheets are more than unidirectional HFRP sheets. Involving two-dimensional weaving technology, the deviation of latitude fiber arrangement leads to the large dispersion of material properties

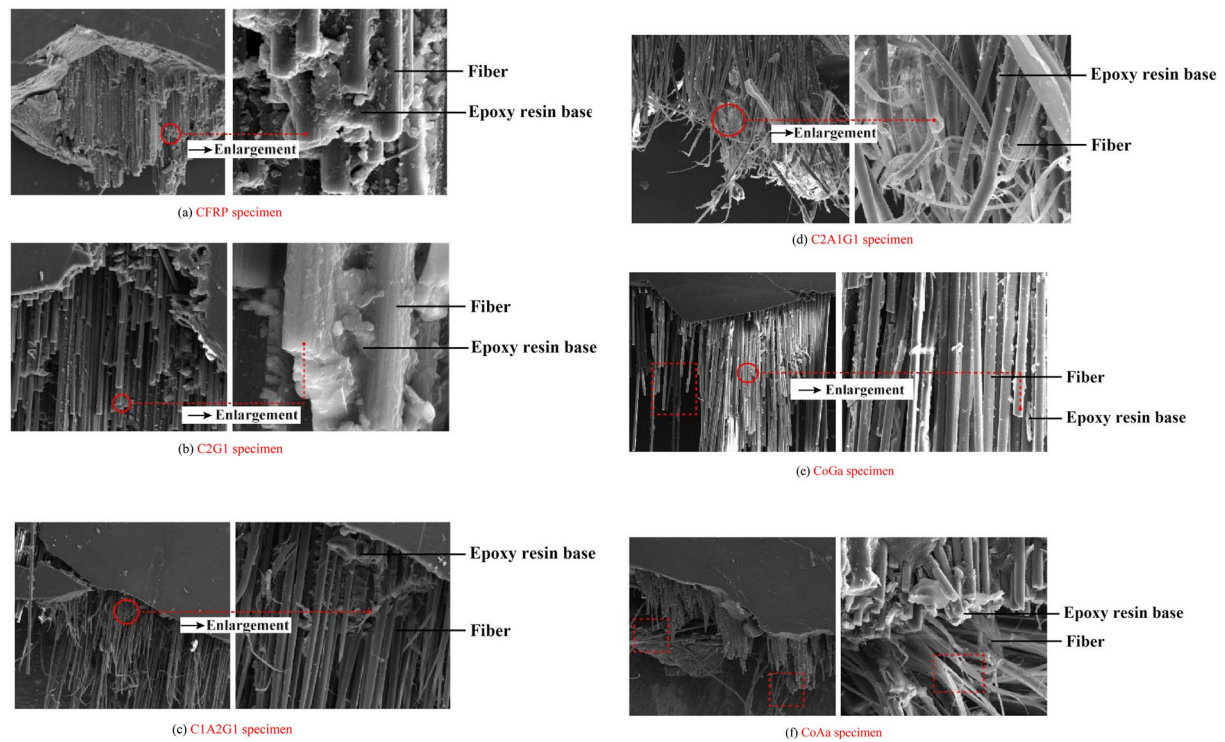
ductility than CFRP; however, its tensile strength was slightly decreased, and the microscopic stress mode was not reasonable. Furthermore, C2G1 behaved similarly to CFRP; its ductility was enhanced, but its strength was slightly reduced, compared to CFRP. The bidirectional sheet provided a more comprehensive advantage than the unidirectional sheet. CoGa has greater tensile strength and a more reasonable stress pattern than CoAa; hence, it was deemed to perform better. The performance of C2A1G1 was better than the other three unidirectional fabrics in material property evaluations, and compared

with the unidirectional sheet, there was a tendency to a better performance of the bidirectional sheet if the cost of the weaving process and other parameters allowed.

#### Timber

*Cunninghamia lanceolata* timber specimens were used in this investigation. Fifty-four specimens were prepared to measure tensile/compressive/shear performance evaluation of six parallel grain, tangential grain, and radial grain. According to the specification



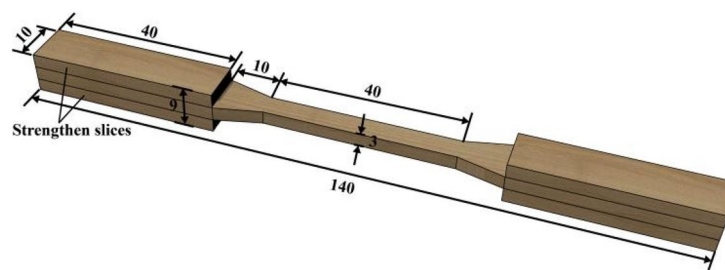


**Fig. 4** Micromorphology of tensile fracture of HFRP specimens

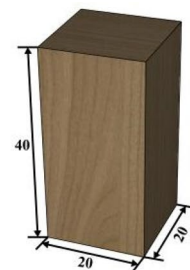
GB/T 1928–2009 [39], all specimens were made from the same batch of timber and were placed in a constant temperature and humidity environment of 20 °C and 65% relative humidity until the moisture content reached  $12 \pm 1\%$ . Dimensions of the compressive specimens were determined according to GB/T 1935–2009 [40] and GB/T 1943–2009 [41], as shown in Fig. 5b. The tensile specimen dimensions were set according to Yoshihara and Ohta's suggestions [42], as shown in Fig. 5a. Shear mechanical properties of

specimens were obtained with shear tests proposed by Iosipescu [43, 44], as shown in Fig. 5c. An asymmetric four-point concentrated load was applied to create a pure shear stress state at the fracture surface, as shown in Fig. 6.

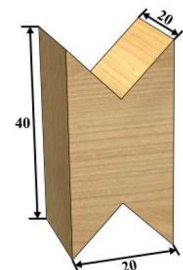
A universal testing machine (Model CMT5504, Mechanical Testing & Simulation System Corporation, United States) was used for the timber material properties test, as shown in Fig. 6. The loading rate was selected as 0.1 mm per minute. Typical damage patterns for the three tests and the average values of the test results are shown in Fig. 7 and Table 4, respectively.



(a) Tensile specimen size



(b) Compressive specimen size



(c) Shear specimen size

**Fig. 5** Test specimens' size of material properties (unit: mm)



Fig. 6 Test devices of material properties

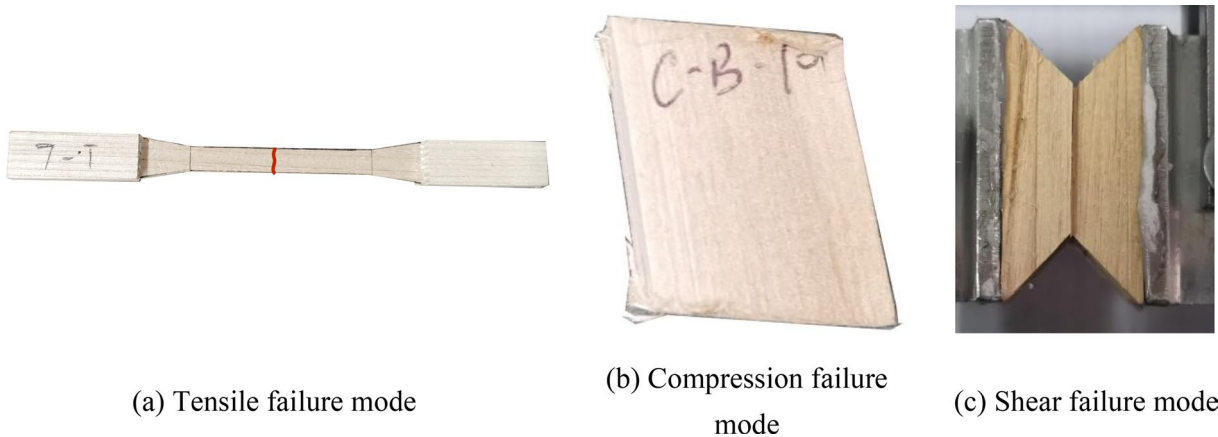


Fig. 7 Failure mode of material property tests

Table 4 Material properties of timber

$E_L$ (MPa)	$E_R$ (MPa)	$E_T$ (MPa)	$\nu_{LR}$	$\nu_{TL}$	$\nu_{RT}$
9167 (7.04)	1100 (4.39)	689 (8.67)	0.35 (6.65)	0.028 (6.44)	0.4 (4.59)
$G_{LR}$ (MPa)	$G_{LT}$ (MPa)	$G_{RT}$ (MPa)	$f_{tL}$ (MPa)	$f_{tR}$ (MPa)	$f_{tT}$ (MPa)
656 (4.76)	600 (8.72)	70 (5.17)	27 (5.27)	3.1 (7.66)	3.2 (5.64)
$f_{cyL}$ (MPa)	$f_{cyR}$ (MPa)	$f_{cyT}$ (MPa)	$f_{LR}$ (MPa)	$f_{LT}$ (MPa)	$f_{RT}$ (MPa)
29 (5.66)	5.5 (4.86)	5.5 (3.29)	5.9 (5.93)	5.8 (7.74)	0.7 (7.35)

Coefficient of variation is in the parentheses, unit: %. Subscript L represents the parallel grain direction, R represents the radial direction, and T represents the tangential direction. The elastic modulus  $E$ , Poisson's ratio  $\nu$ , shear modulus  $G$ , tensile strength  $f_t$ , compressive yield strength  $f_{cy}$ , shear strength  $f_{LR}$ ,  $f_{LT}$  and  $f_{RT}$  can be obtained by strain gauges adhered to the specimens

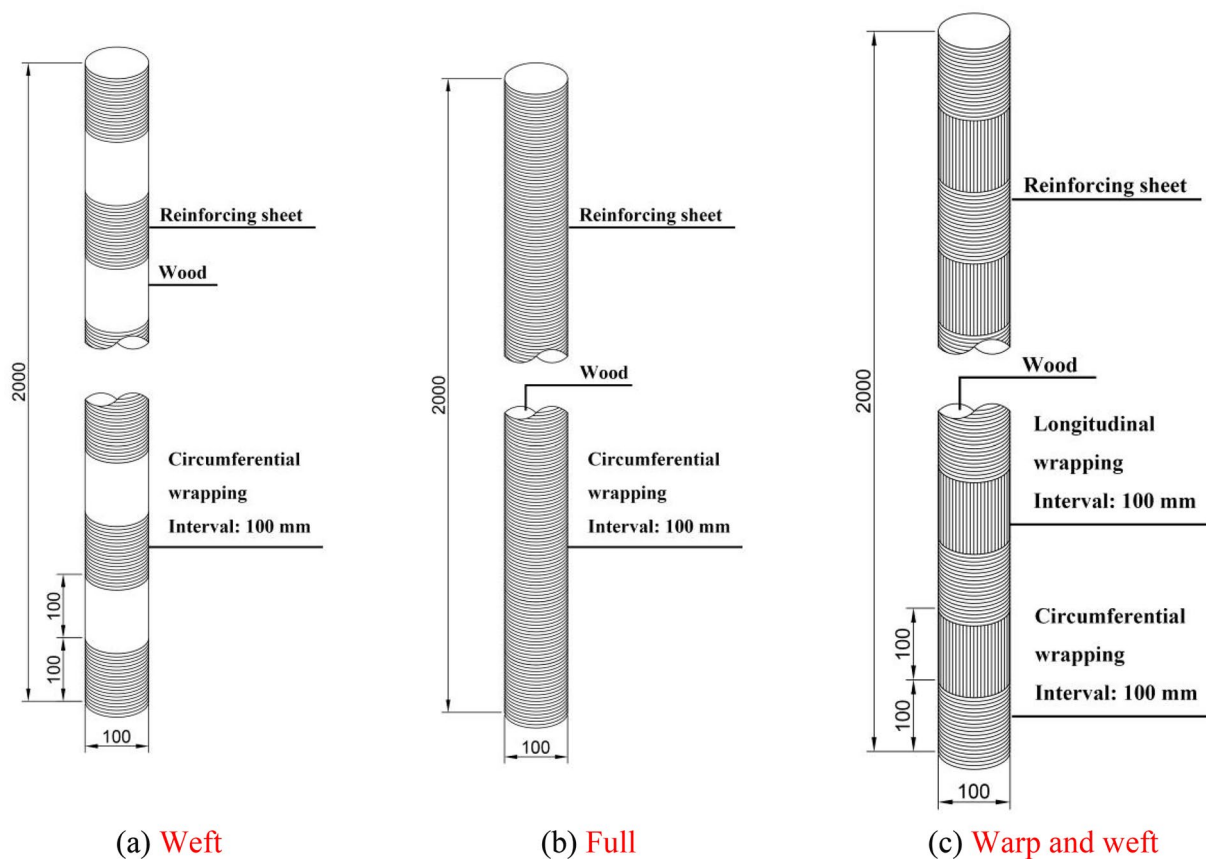
Compression experiments

Test specimens

The HFRP sheets were mounted in three methods, as shown in Fig. 8, to a series of 36 timber columns made of *Cunninghamia lanceolata* with a circular cross section of 100 mm in diameter and 2,000 mm in length. The

first method was 100 mm weft wrapping, divided into reinforced one layer and reinforced two layers with a total of 24 columns, as illustrated in Fig. 8a. Method two was full wrapping, a total of 8 columns, as shown in Fig. 8b. On the other hand, method three involved warp and weft wrapping with 100 mm intervals, as shown





**Fig. 8** The schematic diagram of adhesion methods

in Fig. 8c, a total of 2 columns. Together with the two columns of the control group, a total of 36 columns were used experimental study, as given in Fig. 9.

The compression test process was divided into two parts. The first group of compression tests consisted of timber columns reinforced by the weft wrapping method, six types of HFRP sheets (including single layer reinforcement and double-layer reinforcement), and two unreinforced columns as the control group, a total of 26 columns. The second group of test specimens was C2G1, C2A1G1, and bidirectional HFRP sheets with full wrapping reinforcement, C2A1G1 with warp and weft wrapping reinforcement, and the control group, a total of 20 columns. The serial numbers of the two group specimens are given in Table 5. The following are the naming conventions for compression specimens: the circular section is represented by the first letter "C", the name of the HFRP sheet used for reinforcement is in brackets, the number following the brackets denotes the number of reinforcement layers, and the last "1" or "2" is the specimen number. Individual specimen names beginning with "FL" denote full wrapping reinforcement,

whereas lanceolate "AL" denote weft and warp interval reinforcement.

#### Experimental procedures

The compression experiments were conducted at the Civil Engineering Laboratory of Nanjing University of Aeronautics and Astronautics. The samples were tested using a hydraulic pressure testing machine at a constant loading speed of 0.5 mm/s with displacement control protocol. The boundary conditions were fixed constraints at both ends. The steel plate was mounted at both ends of the test machine after a sleeve slightly greater than the test specimen was welded to it. To measure strain variations, 12 strain gauges were mounted to the column in four groups. Two linear variable differential transducers were placed at each trisecting point, and two were also placed on each side of the column to measure vertical displacement changes. The test equipment, the layout of strain gauges, and linear variable differential transducers are presented in Fig. 10. Once the column failed or the displacement exceeded the measurement range, the loading process was stopped. The load–displacement



**Fig. 9** 36 columns after compression experiment

curves and typical failure modes for the entire process was recorded.

## Results and discussion

### Failure mode

The typical failure modes of the timber column for the compression tests are depicted in Fig. 11. The damage pattern of the unreinforced column was bending damage in the middle of the specimen, which was typical long column destabilization damage, as illustrated in Fig. 11a. After the timber fibers on the tension side of the specimen were pulled off, the horizontal cracks appeared, leading to the final failure of the timber column (the vertical crack in Fig. 11a was a shrinkage crack, which was the initial defect). As shown in Fig. 11b–d, for specimens reinforced by the weft wrapping method with one layer HFRP sheets cracks formed in the central junction region. The bending damage occurred while the other side yielded under pressure. The initial transverse tensile crack was typically located where the reinforced fiber piece and the unreinforced portion intersected; the crack did not extend parallel to the junction but obliquely toward the knots. The failure mode of the specimen reinforced with bidirectional HFRP sheets is presented

in Fig. 11e. Unlike unidirectional sheets, bidirectional sheets reinforced two directions of the column, and the damaged region was not observed in the middle. The bending cracks, influenced by the knots, were produced in the unreinforced area. The cracks generally developed toward the knot grain alteration area. On the other side, compression yielding occurred, and when the entire section was damaged, the column completely failed. Figure 11f depicts the typical failure mode of columns reinforced by the full wrapping method. Due to the wrapping method, the interior timber cracks could only be estimated based on the damage to the HFRP sheets' surface. The right side of the HFRP sheet substrate was damaged, however, the fibers were not completely pulled off. Based upon the evidence of compression on the left side, it can be assumed that the specimen was the same as the above three damage patterns, which were bending damage. The right side was under tension and the left side under compression, while the damaged area was located in the middle of the specimen. Figure 11g demonstrates the typical failure mode of columns reinforced by the warp and weft wrapping method. The left side of the figure has a pressure crack, and the right side has a tension crack, both of which developed in the weft

**Table 5** Timber columns specimens for compression test

Timber column specimen		
Group one		
Control group		
Column without reinforced	C-1	C-2
Type of the reinforced fiber sheet		
CFRP	C-(C)1-1	C-(C)2-1
	C-(C)1-2	C-(C)2-2
C2G1	C-(C2G1)1-1	C-(C2G1)2-1
	C-(C2G1)1-2	C-(C2G1)2-2
C2A1G1	C-(C2A1G1)1-1	C-(C2A1G1)2-1
	C-(C2A1G1)1-2	C-(C2A1G1)2-2
C1A2G1	C-(C1A2G1)1-1	C-(C1A2G1)2-1
	C-(C1A2G1)1-2	C-(C1A2G1)2-2
CoGa	C-(CoGa)1-1	C-(CoGa)2-1
	C-(CoGa)1-2	C-(CoGa)2-2
CoAa	C-(CoAa)1-1	C-(CoAa)2-1
	C-(CoAa)1-2	C-(CoAa)2-2
Group two		
Control group		
Column without reinforced	C-1	C-2
C2G1	C-(C2G1)1-1	C-(C2G1)1-2
C2A1G1	C-(C2A1G1)1-1	C-(C2A1G1)1-2
CoGa	C-(CoGa)1-1	C-(CoGa)1-2
CoAa	C-(CoAa)1-1	C-(CoAa)1-2
Reinforced methods		
Full wrapping	C-FL-(C2A1G1)1-1	C-FL-(C2A1G1)1-2
	C-FL-(CoGa)1-1	C-FL-(CoGa)1-2
	C-FL-(CoAa)1-1	C-FL-(CoAa)1-2
	C-FL-(C2G1)1-1	C-FL-(C2G1)1-2
Interval of longitudinal and latitudinal wrapping	C-AL-(C2A1G1)1-1	C-AL-(C2A1G1)1-2

The letter C in the above table on the left side represents the circular section. The word in the bracket represents the name of the reinforced fiber sheet. The reinforced methods mentioned in Fig. 8 are claimed in the second phase in the numbers. FL, AL corresponding method two and method three, respectively. And Besides the letter C, if there is no word before the bracket, it is representing method one. the number outside the bracket represents the number of layers, and the last number represents the number of repeated specimens. For example, C-FL-(CoGa)1-2 represents the second specimen of the group with round cross section, the reinforced method is full wrapped with CoGa bidirectional hybrid fiber sheet, and the number of the layer is one

reinforced section in the middle of the specimen, as the completely wrapped specimens. The cracks on the left were triangular, which may be related to a sudden change in the texture of the timber knots and the possibility of triggering irregular crack formation.

The cracks were usually located in the middle region of the sample, but a slight deviation trend was detected in a few samples. The location of the knot was substantially correlated with the direction of crack expansion. In

addition, a complete shear fracture was not detected in the samples; hence, shear reinforcement did not play a better strengthening effect. The development of the reinforcement method for the compressive performance of columns will continue to be discussed.

#### Load–displacement curve

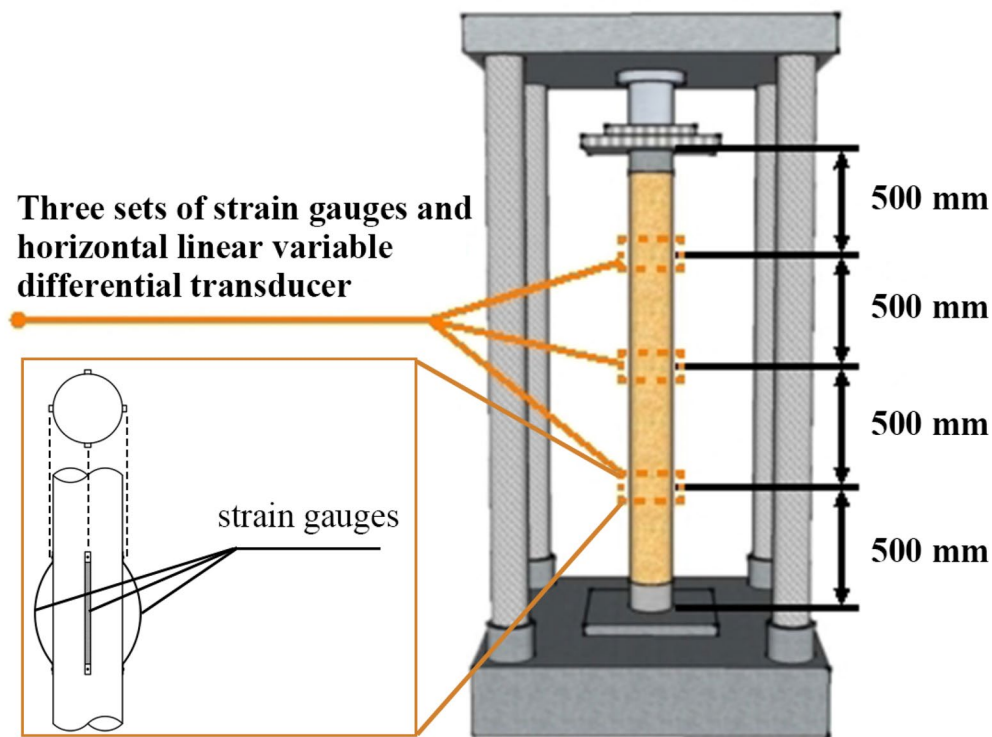
The load–displacement curves of the seven specimen groups, including the unreinforced control group, are presented in Fig. 12, and the statistics of the experimental results are presented in Table 6.

The displacements correspond to the relative vertical displacements in the middle part. Among them, the bearing capacity and displacement of C-(C1A2G1)2-1 and C-(CoAa)2-2 are less than those of the unreinforced columns. These unreasonable results are mainly due to the timber knots and the cross grain. Therefore, these sets of data were excluded in the subsequent analysis. The coefficient of variation of unreinforced columns in terms of ultimate bearing capacity was 4.29%, while the highest coefficient of variation in the experiment was 6.28% for C2A1G1. In general, columns reinforced with the same HFRP sheet exhibited reduced dispersion and fewer outliers in their bearing capability. Furthermore, the number of latitudinal reinforcement layers had no significant effect on the ultimate bearing capacity of the columns. The findings also revealed that the selection of the same timber batch ensures that the compressive capacity of the columns is essentially similar, despite the effects of shrinkage cracks and knots. Therefore, the averaged test results reflected the general regular trend, except for individual discrete values.

The unreinforced columns have some ductility in terms of ductility. Moreover, after attaining ultimate bearing capacity, the load gradually reduced to around 80% of ultimate bearing capacity as displacement increased, and test specimens eventually failed rapidly.

Figure 13 shows the load–displacement curves of the second group of experiments. The bearing capacity and displacement of C-FL-CoAa-2 are less than those of the unreinforced columns. These unreasonable results are mainly due to the timber knots and the cross grain. Therefore, this set of data was excluded in the subsequent analysis. From Fig. 13, compared with the other two reinforcement methods, the enhancement of ultimate bearing capacity by full wrapping was the largest. The increase in bearing capacity achieved by the warp and weft interval wrapping method had a tendency to be less than that achieved by full wrapping reinforcement but greater than that achieved by weft interval reinforcement. Furthermore, the ductility improvement attained by these two approaches was nearly identical to that





**Fig. 10** Test device and layout of measurements

attained by weft interval reinforcement, and the length of nonlinear decrease and displacement at ultimate failure were essentially equal.

### Discussion

The displacement corresponding to the ultimate bearing capacity was defined as the ultimate displacement. The difference between the displacement when the timber column completely failed (the bearing capacity decreased to less than 50% of the ultimate bearing capacity) and the ultimate displacement was defined as the softening displacement. The rate of increase in ultimate bearing capacity, ultimate displacement, and softening displacement was calculated for each reinforced group, compared to the unreinforced group. The bearing capacity of columns reinforced with different types of HFRP sheets in weft interval wrapping, and also improvement of the bearing capacity of columns reinforced with various reinforcement methods, are examined in this section.

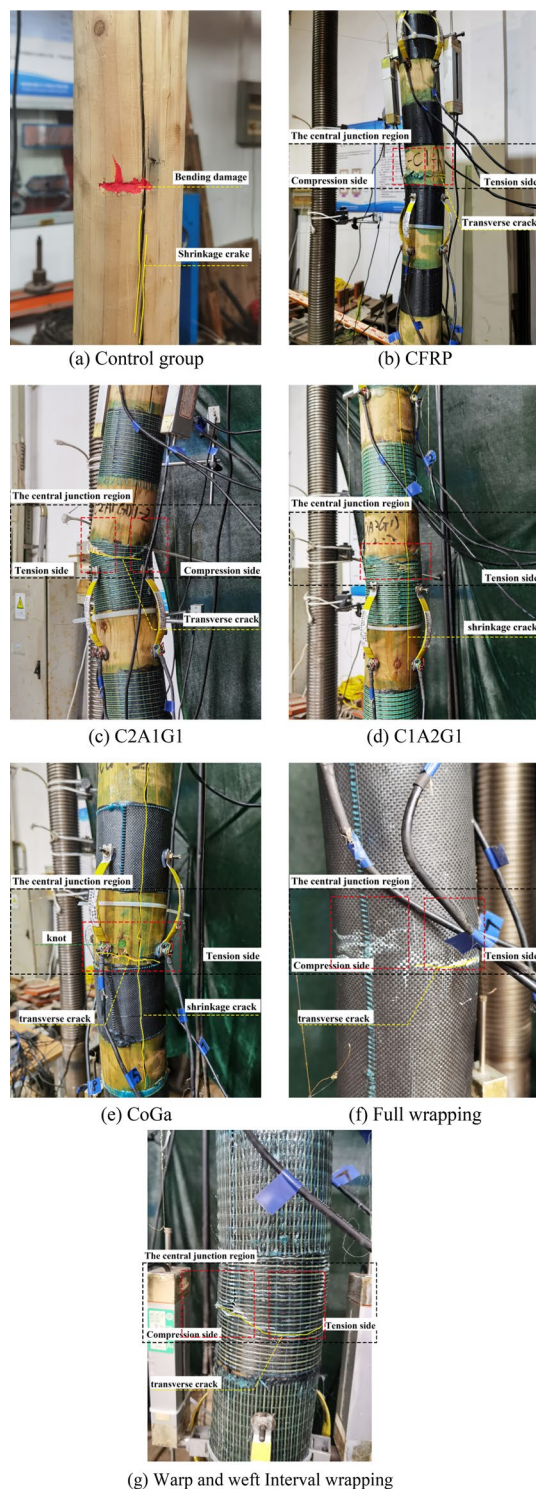
### Types of HFRP sheets

Unidirectional sheets with weft interval reinforcement could improve the compressive performance of the timber column; however, the ultimate bearing capacity improvement was relatively limited, and the range was

detected as 4.47–11.06% (Fig. 14a). The ultimate bearing capacity was improved by 7.41% when a CFRP sheet was used for reinforcement. Besides that, the reinforcement effect of C2G1 and C1A2G1 was 0.23–2.95% lower than that of CFRP, which also can be considered to be similar with the reinforcement effect of CFRP. These small differences possibly due to the sheer volume of low-strength fibers added and the rather poor stress distribution after compounding. C2A1G1 had the best improvement for ultimate bearing capacity among the four unidirectional sheets, at 10.12%. It might be attributed to the tight fiber arrangement, the stronger carbon fiber filaments act as a lateral restraint to the aramid fibers and glass fibers, thus generating a better stress pattern, consistent with the material test findings.

According to the ductility performances, as shown in Fig. 14b, c, CFRP and C2G1 showed similar improvement, with the ultimate displacement enhancement of around 90–100% and the softening displacement enhancement of around 320–360%. Among the four unidirectional sheets, C2A1G1 exhibited the best overall performance of the four unidirectional sheets, with a 374.89% in ultimate displacement and a considerable improvement in softening displacement.

The improvement in the ultimate bearing capacity of columns with bidirectional sheets was significant,



**Fig. 11** Typical failure modes of timber columns

ranging from 16.93–23.18%, with CoGa providing slightly better reinforcement than CoAa, as shown in Fig. 14a. The improved compressive bearing capacity of columns

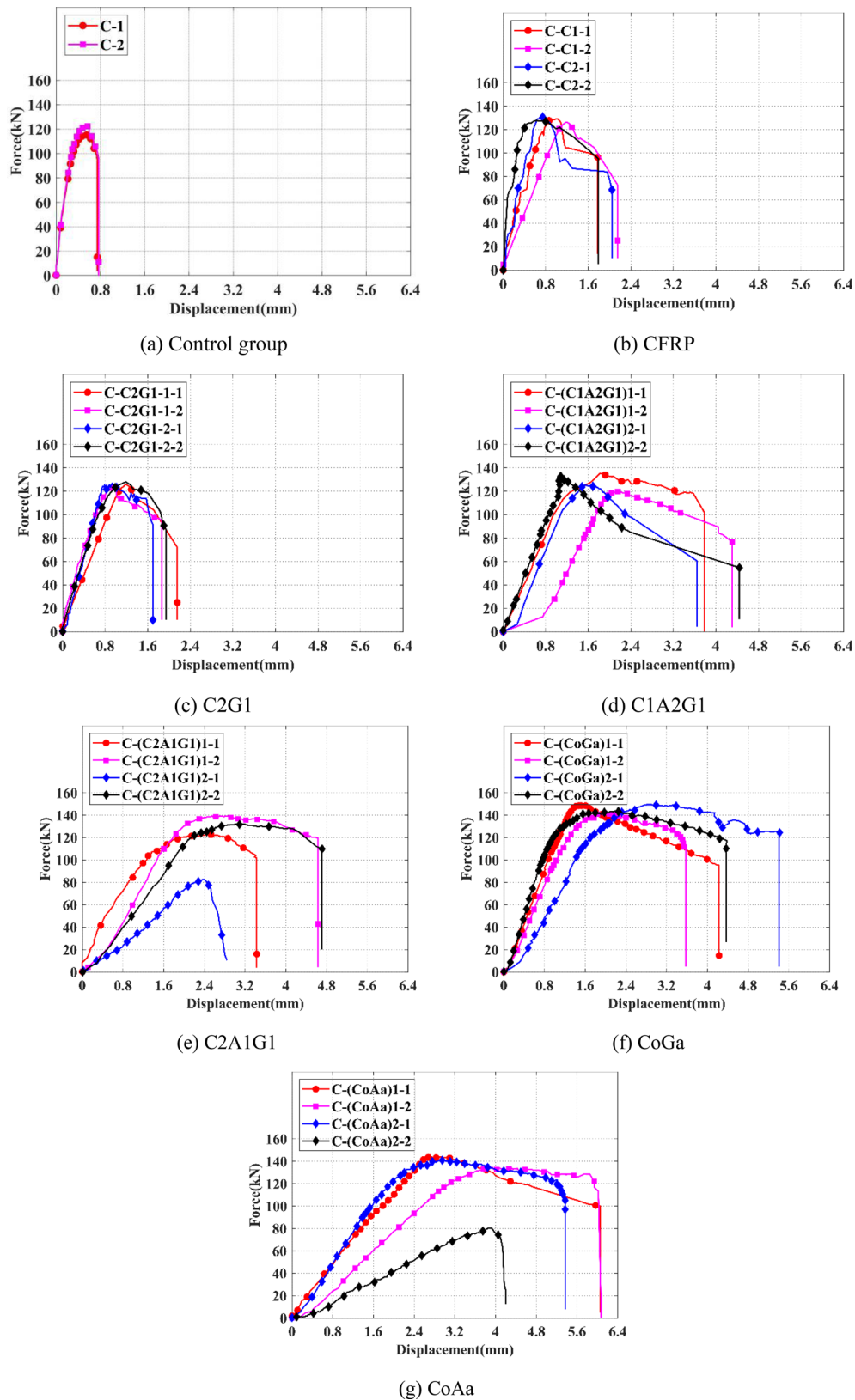
by a single layer of CoGa reached about 22.27%. The reason behind this was that the bidirectional sheets had reinforcing fibers in both the warp and weft directions. The warp fibers enhanced the bending resistance of the column, while the weft fibers provided circular restraint, inhibits the expansion of timber fibers; thus, the compression resistance of the column increased. This was an advantage that the bidirectional sheet possessed. The glass fibers were stronger than the aramid fibers. In terms of ductility, as shown in CoAa showed better performance between the two bidirectional sheets as shown in Fig. 14b, c, since the aramid fibers in the weft direction were tough, which greatly increased the ductility of the columns. Therefore, the improvement in the ultimate displacement of CoGa was positioned between C1A2G1 and C2A1G1.

Furthermore, a slight improvement was observed in the general performance of two layers compared to one layer with a 0.91–5.35%. The softening displacement of reinforcing two layers of CoAa sheets and C2G1 sheets was less than that of reinforcing one layer, indicating that the increase in ductility by reinforcing two layers will not result in a significant improvement. This output could be attributed to more factors affecting the softening displacement, increasing the dispersion to a certain extent.

#### Methods of reinforcement

In Fig. 15, 'FL' represents full wrapping reinforcement, 'WL' represents weft interval reinforcement, and 'AL' represents warp–weft interval reinforcement. In Fig. 15a, full wrapping reinforcement had the greatest improvement on the bearing capacity, compared to the weft interval reinforcement, C2G1 increased 18.59% and C2A1G1 increased 16.61% in the unidirectional sheets. However, the improvement is not much for the bidirectional sheets, only 7.09% for CoGa, and 9.98% for CoAa, both less than 10%. In Fig. 15a, full wrapping reinforcement had the most remarkable improvement on the bearing capacity; compared to the weft interval reinforcement, C2G1 increased by 18.59%, and C2A1G1 increased by 16.61% in the unidirectional sheets.

In terms of ductility, as shown in Fig. 15b, c, full wrapping reinforcement did not improve much compared to the other two reinforcement methods, so the results for the CoAa group were not included. It can be seen that the bidirectional sheet full wrapping reinforcement was not better than the interval reinforcement. Therefore, the interval wrapping reinforcement would have a positive impact, and the sheet's area would be decreased by nearly half. The improvement in ductility of timber columns using the two additional C2A1G1 warp and weft interval reinforcement test groups was remarkably similar to

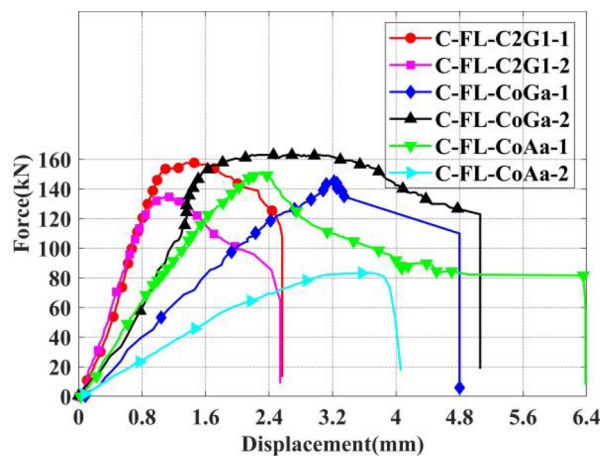
**Fig. 12** Load–displacement curve of group one



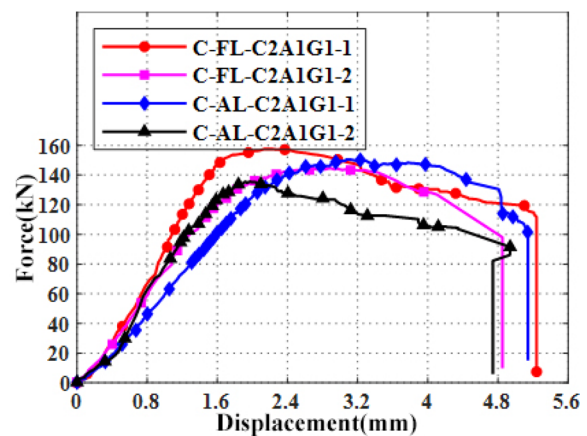
**Table 6** Results of compression tests

Material parameter	Control group	(CFRP)1	(C2G1)1	(C1A2G1)1	(C2A1G1)1	(CoGa)1	(CoAa)1
The ultimate bearing capacity	119.06 (kN)	127.88 kN	124.37 kN	127.62 kN	131.11 kN	145.76 kN	139.38 kN
The increasing rate	\	7.40%	4.46%	7.18%	10.12%	22.42%	17.06%
The ultimate displacement	0.550 (mm)	1.108 mm	1.060 mm	1.973 mm	2.610 mm	1.700 mm	3.309 mm
The increasing rate	\	101.53%	92.89%	259.06%	374.89%	209.42%	502.20%
The softening displacement	0.755 (mm)	1.965 mm	2.008 mm	4.041 mm	4.026 mm	3.900 mm	6.066 mm
The increasing rate	\	160.44%	166.07%	435.59%	433.60%	416.90%	703.91%
Material parameter	Control group	(CFRP)2	(C2G1)2	(C1A2G1)2	(C2A1G1)2	(CoGa)2	(CoAa)2
The ultimate bearing capacity	119.06 (kN)	129.25 kN	127.43 kN	129.01 kN	132.24 kN	146.66 kN	141.34 kN
The increasing rate	\	8.55%	7.02%	8.35%	11.07%	23.18%	18.71%
The ultimate displacement	0.559 (mm)	0.683 mm	1.063 mm	1.308 mm	3.042 mm	2.488 mm	2.944 mm
The increasing rate	\	22.18%	90.21%	134.14%	444.49%	345.31%	426.99%
The softening displacement	0.767 (mm)	1.913 mm	1.822 mm	4.044 mm	4.711 mm	4.909 mm	5.366 mm
The increasing rate	\	205.16%	188.78%	586.65%	706.05%	741.50%	823.31%

The ultimate bearing capacity, ultimate displacement, and the softening displacement in the table are the mean value of the test. For C2A1G1 and CoAa, C-(C1A2G1)2-1 and C-(CoAa)2-2 are excluded in the analysis



(a) Full wrapping



(b) Interval wrapping

**Fig. 13** Load-displacement curve of group two

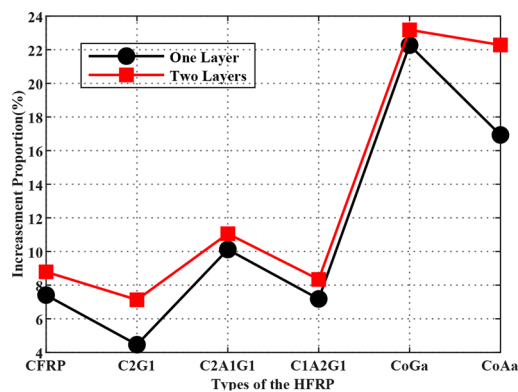
the fully wrapping reinforcement. While the bearing capacity is not much different, the warp and weft interval reinforcement is also a viable technique of reinforcement. Although the area of reinforcement is the same as full wrap reinforcement, this method can make good use of the edges, thus greatly reduce the fiber consumption.

## Conclusions

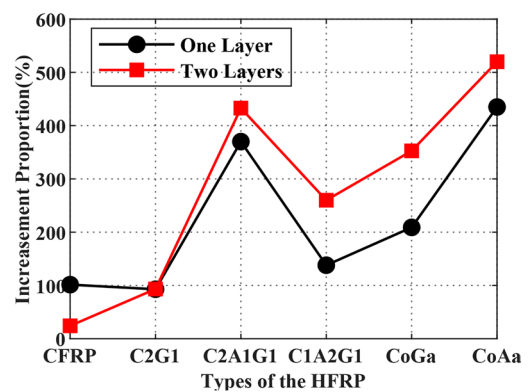
The current study investigated the compressive performance of long timber columns reinforced with HFRP sheets, previously examined in limited. To identify the most suitable carbon fiber, glass fiber, and aramid fiber ratios in unidirectional sheets, researchers analyzed the effects of different blending ratios on the

mechanical characteristics of HFRP sheets. For this purpose, pressure tests were carried out on 36 timber columns and the damage model of long timber columns under compression was discussed. Finally, the impacts of different sheets and reinforcement methods on the compressive performance of long timber columns were investigated, and the following conclusions were reached:

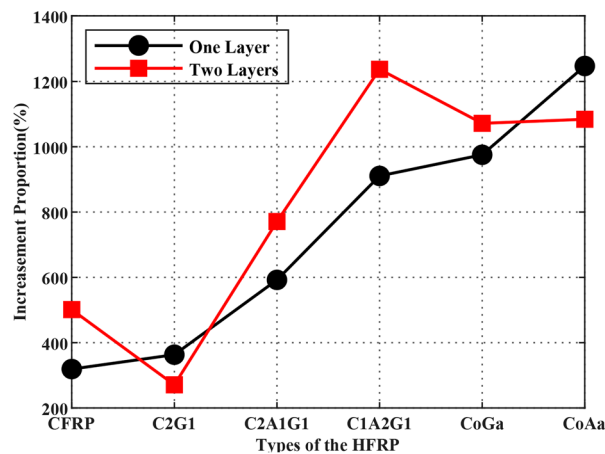
- (1) The bidirectional HFRP sheet performed admirably in the compressive test of reinforced timber columns. The bidirectional HFRP sheet was equivalent to reinforcing both bending and compression resistances of timber columns due to the presence of reinforcing fibers in both warp and



(a) Ultimate bearing capacity



(b) Ultimate displacement



(c) Softening displacement

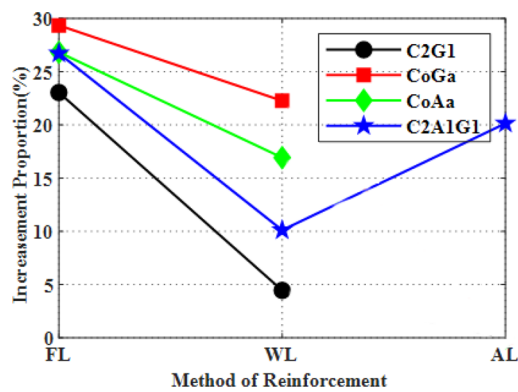
**Fig. 14** The effect of different sheet types and different reinforced layer

weft directions. The bearing capacity improvement with single layer CoGa interval reinforcement reached 22.27%, which is three to five times larger than that of a unidirectional sheet. In contrast, the sheet area was only half of that with full wrapping reinforcement, which significantly reduced material consumption. The weft fiber of the bidirectional sheet was proposed to use glass fiber, relying on the microscopic stress pattern and experimental results.

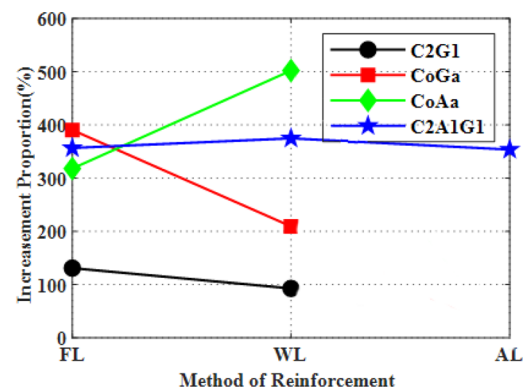
- (2) The full wrap reinforcement was responsible for the greatest improvement in the compression performance of the timber column, while the weft reinforcement was slightly less effective than the full wrap reinforcement. For the unidirectional sheet, the reinforcement effect was reduced by about 50%, while the reduction rate was about 25% for the bidirectional sheet. The patching area of weft

interval reinforcement was only half of that of full wrapping reinforcement. Furthermore, warp and weft interval reinforcement proved to be a better method of reinforcement. C2A1G1 warp–weft interval reinforcement was about twice as good as weft interval reinforcement, and it was 6.58% lower compared to full wrapping reinforcement. And all three methods have greatly improved the ductility of timber columns compression behavior, changing the brittle damage when the timber columns under pressure. Consequently, it has been demonstrated by the findings that this reinforcement method can be well adapted to the practical application in timber structures if the cost is not taken into consideration.

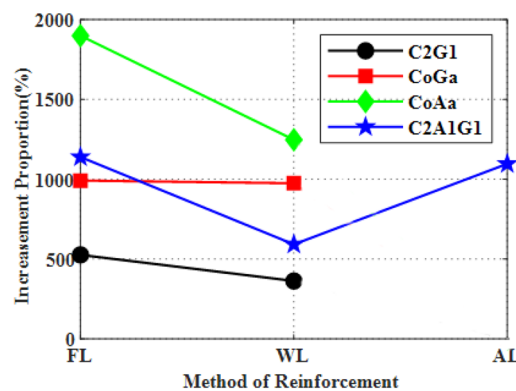
- (3) It has been found that using an HFRP sheet to reinforce timber columns can improve the compressive bearing capacity of the column.



(a) Ultimate bearing capacity



(b) Ultimate displacement



(c) Softening displacement

**Fig. 15** The effect of different reinforced methods

The improving range was found at 4.46–29.36%, depending on the reinforcement method and reinforcing sheet. In addition, it was found that the externally wrapping HFRP sheet significantly improved the ductility of the timber column. The improvement of ultimate displacement was measured as 92.88–502.20%. Among the four unidirectional sheets, C2A1G1 exhibited the best performance. The bearing capacity improvement by full wrapping reinforcement was detected at 26.73%, while for warp and weft interval reinforcement it was detected at 20.15%. Furthermore, the ductility enhancement was slightly less than C1A2G1, significantly better than other unidirectional sheets.

CFRP Carbon fiber reinforced polymers  
AFRP Aramid fiber reinforced polymers  
BFRP Basalt fiber reinforced polymers  
GFRP Glass fiber reinforced polymers

#### Acknowledgements

Not applicable.

#### Author contributions

HW contributed to the methodology, simulation, results analysis, and original draft of this manuscript. QC contributed to review of this manuscript. All authors contributed to the experiments. All authors read and approved the final manuscript.

#### Funding

This research was supported by the National Nature Science Foundation of China (Grant No. 51778122), and the Research and development project of China State Construction Engineering Corporation (Grant No. CSCEC-2021-Z-36).

#### Availability of data and materials

The datasets used and/or analyzed during the current study are available from the corresponding author on reasonable request.

#### Abbreviations

FRP Fiber-reinforced polymers  
HFRP Hybrid fiber reinforced polymers  
SEM Scanning electron microscopy



## Declarations

### Competing interests

The authors declare that they have no competing interests.

Received: 14 July 2022 Accepted: 5 January 2023

Published online: 17 January 2023

## References

- Fernando D, Teng JG, Gattas J, Heitzmann M (2018) Hybrid fibre-reinforced polymer-timber thin-walled structural members. *Adv Struct Eng* 21:1409–1417. <https://doi.org/10.1177/1369433217739709>
- Bai W, Moustafa MA, Dai JW, Yang YQ, Du K, Chen XZ (2021) Damage assessment of Shuanghe Confucian temple after Changning earthquake mainshock and aftershocks series. *B Earthq Eng* 19:5977–6001. <https://doi.org/10.1007/s10518-021-01207-9>
- Cestari CB, Marzi T (2018) Conservation of historic timber roof structures of Italian architectural heritage: diagnosis, assessment, and intervention. *Int J Archit Herit* 12:632–665. <https://doi.org/10.1080/15583058.2018.1442523>
- Santini S, Baggio C, Sguerri L (2021) Sustainable interventions: conservation of old timber roof of Michelangelo's cloister in Diocletian's baths. *Int J Archit Herit*. <https://doi.org/10.1080/15583058.2021.1938747>
- Cavalli A, Cibecchini D, Togni M, Sousa HS (2016) A review on the mechanical properties of aged wood and salvaged timber. *Constr Build Mater* 114:681–687. <https://doi.org/10.1016/j.conbuildmat.2016.04.001>
- ICOMOS (International Council on Monuments and Sites) (2015) Principles for the conservation of heritage sites in China (revised 2015), Cultrural Relics Press, Beijing
- Franke S, Franke B, Harte AM (2015) Failure modes and reinforcement techniques for timber beams—state of the art. *Constr Build Mater* 97:2–13. <https://doi.org/10.1016/j.conbuildmat.2015.06.021>
- Ling ZB, Liu WQ, Shao JS (2020) Experimental and theoretical investigation on shear behaviour of small-scale timber beams strengthened with fiber-reinforced polymer composites. *Compos Struct* 240. <https://doi.org/10.1016/j.compstruct.2020.111989>
- Gupta MK, Srivastava RK (2016) Mechanical properties of hybrid fibers-reinforced polymer composite: a review. *Polym-plast Technol* 55:626–642. <https://doi.org/10.1080/03602559.2015.1098694>
- Garcia PD, Escamilla AC, Garcia MNG (2013) Bending reinforcement of timber beams with composite carbon fiber and basalt fiber materials. *Compos Part B Eng* 55:528–536. <https://doi.org/10.1016/j.compositesb.2013.07.016>
- Liu JA, Dong ZQ, Zhu XY, Sun WB, Huang ZQ (2022) Flexural properties of lightweight carbon fiber/epoxy resin composite sandwiches with different fiber directions. *Mater Res Express* 9. <https://doi.org/10.1088/2053-1591/ac4dc5>
- Davies IJ, Hamada H (2001) Flexural properties of a hybrid polymer matrix composite containing carbon and silicon carbide fibres. *Adv Compos Mater* 10:77–96. <https://doi.org/10.1163/15685510152546376>
- Yang H, Song HW, Zhang S (2015) Experimental investigation of the behavior of aramid fiber reinforced polymer confined concrete subjected to high strain-rate compression. *Constr Build Mater* 95:143–151. <https://doi.org/10.1016/j.conbuildmat.2015.07.084>
- Singh J, Kumar M, Kumar S, Mohapatra SK (2017) Properties of glass-fiber hybrid composites: a review. *Polym-plast Technol* 56:455–469. <https://doi.org/10.1080/03602559.2016.1233271>
- Giridharan R (2019) Preparation and property evaluation of Glass/Ramie fibers reinforced epoxy hybrid composites. *Compos Part B Eng* 167:342–345. <https://doi.org/10.1016/j.compositesb.2018.12.049>
- Ghani AFA, Mahmud J (2017) Shear deformation behavior of hybrid composite (GFRP/CFRP). *Materialwiss Werkst* 48:273–282. <https://doi.org/10.1002/mawe.201600771>
- Sapuan SM, Aulia HS, Ilyas RA, Atiqah A, Dele-Afolabi TT, Nurazzi MN, Suian ABM, Atikah MSN (2020) Mechanical properties of longitudinal basalt/woven-glass-fiber-reinforced unsaturated polyester-resin hybrid composites. *Polymers (Basel)* 12. <https://doi.org/10.3390/polym12102211>
- Umashankaran M, Gopalakrishnan S, Sathish S (2020) Preparation and characterization of tensile and bending properties of basalt-kenaf reinforced hybrid polymer composites. *Int J Polym Anal Ch* 25:227–237. <https://doi.org/10.1080/1023666x.2020.1781480>
- Gomez EP, Gonzalez MN, Hosokawa K, Cobo A (2019) Experimental study of the flexural behavior of timber beams reinforced with different kinds of FRP and metallic fibers. *Compos Struct* 213:308–316. <https://doi.org/10.1016/j.compstruct.2019.01.099>
- Hayajneh M, Al-Oqla FM, Aldhirat A (2022) Physical and mechanical inherent characteristic investigations of various Jordanian natural fiber species to reveal their potential for green biomaterials. *J Nat Fibers*. <https://doi.org/10.1080/15440478.2021.1944432>
- Bozkurt OY, Erklig A, Bulut M (2018) Hybridization effects on Charpy impact behavior of basalt/aramid fiber reinforced hybrid composite laminates. *Polym Composite* 39:467–475. <https://doi.org/10.1002/pc.23957>
- Wang B, Bachtar EV, Yan LB, Kasal B, Fiore V (2019) Flax, basalt, E-glass FRP and their hybrid FRP strengthened wood beams: an experimental study. *Polymers (Basel)* 11. <https://doi.org/10.3390/polym11081255>
- Baghi H, Barros JAO, Ventura-Gouveia A (2016) Shear strengthening of reinforced concrete beams with hybrid composite plates. *Adv Struct Eng* 19:132–155. <https://doi.org/10.1177/1369433215622873>
- Attari N, Amziane S, Chemrouk M (2012) Flexural strengthening of concrete beams using CFRP, GFRP and hybrid FRP sheets. *Constr Build Mater* 37:746–757. <https://doi.org/10.1016/j.conbuildmat.2012.07.052>
- Ferrier E, Labossiere P, Neale KW (2012) Modelling the bending behaviour of a new hybrid glulam beam reinforced with FRP and ultra-high-performance concrete. *Appl Math Model* 36:3883–3902. <https://doi.org/10.1016/j.apm.2011.11.062>
- Rescalvo FJ, Suarez E, Abarkane C, Cruz-Valdivieso A, Gallego A (2019) Experimental validation of a CFRP laminated/fabric hybrid layout for retrofitting and repairing timber beams. *Mech Adv Mater Struc* 26:1902–1909. <https://doi.org/10.1080/15376494.2018.1455940>
- Al-Fasih MYM, Mokhtar NI, Ahmad Y, Bin Ibrahim IS, Abu Hassan S (2021) Shear performance of strengthened timber beam with intermittent GFRP strips. *Constr Build Mater* 312. <https://doi.org/10.1016/j.conbuildmat.2021.125394>
- Najm H, Secaras J, Balaguru P (2007) Compression tests of circular timber column confined with carbon fibers using inorganic matrix. *J Mater Civil Eng* 19:198–204. [https://doi.org/10.1061/\(asce\)0899-1561\(2007\)19:2\(198\)](https://doi.org/10.1061/(asce)0899-1561(2007)19:2(198))
- Ouyang Y, Yang X, Bao RH (2011) Nonlinear stability of timber column strengthened with fiber reinforced polymer. *Appl Math Mech-Engl* 32:903–916. <https://doi.org/10.1007/s10483-011-1468-7>
- Xiong XY, Su ZY (2015) Experimental study and theoretical analysis of carbon fibre-reinforced polymer strengthening timber pier column. *Mater Res Innov* 19:1246–1254. <https://doi.org/10.1179/1432891714z.000000001288>
- Siha A, Zhou CD, Yang LG (2021) Experimental study on axial compression behavior on circular timber columns strengthened with CFRP strips and near-surface mounted steel bars. *J Struct Eng* 147. [https://doi.org/10.1061/\(asce\)st.1943-541x.0002931](https://doi.org/10.1061/(asce)st.1943-541x.0002931)
- Dong JF, Yuan SC, Wang QY, Liang W (2015) Influence of fractured wood texture on structural behaviour of timber columns with fibre reinforced polymer reinforcement. *Mater Res Innov* 19:546–550. <https://doi.org/10.1179/1432891714z.0000000001149>
- Lee IH, Song YJ, Hong SI (2021) Evaluation of the compression strength performance of fiber-reinforced polymer (FRP) and steel-reinforced laminated timber composed of small-diameter timber. *Bioresources* 16:633–642. <https://doi.org/10.15376/biores.16.1.633-642>
- Dong JF, Jia P, Yuan SC, Wang QY (2015) Compressive behaviours of square timber columns reinforced by partial wrapping of FRP sheets. *Mater Res Innov* 19:S465–S468. <https://doi.org/10.1179/1432891715z.0000000001593>
- Taheri F, Nagaraj M, Khosravi P (2009) Buckling response of glue-laminated columns reinforced with fiber-reinforced plastic sheets. *Compos Struct* 88:481–490. <https://doi.org/10.1016/j.compstruct.2008.05.013>
- Zhang WP, Song XB, Gu XL, Tang HY (2012) Compressive behavior of longitudinally cracked timber columns retrofitted using FRP sheets. *J*

Struct Eng 138:90–98. [https://doi.org/10.1061/\(asce\)st.1943-541x.0000423](https://doi.org/10.1061/(asce)st.1943-541x.0000423)

37. Lu WD, Wang L, Wu JJ, Liu WQ, Yang HF, Yue K, Chen XW, Sun XL, Deng ZX (2016) Behavior of glulam columns reinforced by near-surface-mounted CFRP laminates under eccentric compression loading. *J Struct Eng* 142. [https://doi.org/10.1061/\(asce\)st.1943-541x.0001585](https://doi.org/10.1061/(asce)st.1943-541x.0001585)
38. GB/T 3354–2014 (2014) Test method for tensile properties of orientation fiber reinforced polymer matrix composite materials. Chinese Standards Press, Beijing (in Chinese)
39. GB/T 1928–2009 (2009) General requirements for physical and mechanical tests of wood. Chinese Standards Press, Beijing (in Chinese)
40. GB/T 1935–2009 (2009) Methods of testing in compressive strength parallel to grain of wood. Chinese Standards Press, Beijing (in Chinese)
41. GB/T 1943–2009 (2009) Method for determination of the modulus of elasticity in compression perpendicular to grain of wood. Chinese Standards Press, Beijing (in Chinese)
42. Yoshihara H, Ohta M (2000) Estimation of the shear strength of wood by uniaxial-tension tests of off-axis specimens. *J Wood Sci* 46:159–163. <https://doi.org/10.1007/bf00777364>
43. Yoshihara H, Ohsaki H, Kubojima Y, Ohta M (1999) Applicability of the losipescu shear test on the measurement of the shear properties of wood. *J Wood Sci* 45:24–29. <https://doi.org/10.1007/bf00579520>
44. Zhang L, Yang N (2017) Evaluation of a modified losipescu shear test method for determining the shear properties of clear wood. *Wood Sci Technol* 51:323–343. <https://doi.org/10.1007/s00226-016-0888-z>

## Publisher's Note

Springer Nature remains neutral with regard to jurisdictional claims in published maps and institutional affiliations.

**Submit your manuscript to a SpringerOpen<sup>®</sup> journal and benefit from:**

- Convenient online submission
- Rigorous peer review
- Open access: articles freely available online
- High visibility within the field
- Retaining the copyright to your article

---

Submit your next manuscript at ► [springeropen.com](https://www.springeropen.com)